Current Opinion in Solid State and Materials Science 11 (2007) 41–46

Contents lists available at ScienceDirect

Current Opinion in Solid State and Materials Science

journal homepage: www.elsevier.com/locate/cossms

The effect of thermodynamic variables on polymer chain dynamics

C.M. Roland

Naval Research Laboratory, Chemistry Division, Code 6120, Washington, DC 20375-5342, United States

ARTICLE INFO

Article history:
Received 16 April 2008
Accepted 18 April 2008

Keywords:
Segmental relaxation
Dielectric spectroscopy
Time-temperature superpositioning
Thermodynamic scaling

ABSTRACT

The dynamics of polymer chains are examined in terms of their relationship to the local segmental relaxation process. Although the differing responses to changes in temperature and pressure cause breakdown of time-temperature and time-pressure superpositioning near the glass transition, a recently discovered scaling law can be applied to both relaxation modes. This scaling yields master curves of the global chain relaxation times and the local segmental relaxation times, which can be used to determine the dynamics at high pressure from ambient pressure measurements. The scaling relation also provides a measure of the steepness on the intermolecular potential in the vicinity of the distance of closest approach between segments.

Published by Elsevier Ltd.

1. Background

The low frequency motions of high molecular weight (“entangled”) polymers are directly relevant to processing and forming operations and exert a substantial influence on many material properties. The conceptual framework of theoretical studies of the dynamics of entangled chains is invariably the reptation model [1,2], which has been widely accepted in view of its intuitive appeal and reasonable agreement with experimental results [3,4]. Where predictions of the reptation model are wrong, this usually implies that mechanisms other than longitudinal (“snakelike”) diffusion are operative [5].

An important aspect of the rheology of polymers is the effect of temperature or pressure on the dynamics. According to the reptation model, at short times the chain segments move freely within a tube of their entanglement constraints. Thus, the motion can be described by the Rouse model [6], which terminates when entanglements begin to manifest themselves. There are two species-dependent parameters, the local (Rouse) friction coefficient, ς, and a parameter characterizing the entanglement effect, so that the temperature dependence of the chain dynamics is governed entirely by ς. Since ς is the same as the local friction coefficient for the segmental motion, the T-dependence of the entire dynamics of a polymer from the glass transition zone to the terminal flow regime are predicted to be the same. This leads to the well-known time-temperature superposition principle, by which master curves of viscoelastic properties are constructed, encompassing many decades of time or frequency, from data measured over a much narrower range [6].

Although time-temperature superpositioning is common and often useful, when the data extend into the glass transition (or softening) zone, polymers exhibit thermorheological complexity. The chain dynamics invariably have a weaker dependence on temperature than the local segmental modes underlying the onset of glassy behavior; this causes deviations from time-temperature superpositioning. First discovered in polystyrene by Plazek [7], this breakdown of the superposition principle is observed in all polymers for which data have been obtained under conditions such that both the chain and the local segmental modes simultaneously contribute (i.e., the glass transition zone): poly(vinyl acetate) [8], polypropylene glycol [9], poly(phenylmethylsiloxane) [10], polyisoprene [11], polybutadiene [12], polyisobutylene [13], atactic polypropylene [14], poly(alkyl glycidyl ether) [15], and *atatic* polypropylene [16]. Well above the glass transition, time constants for the chain dynamics and local segmental relaxation are proportional, so that viscoelastic data time-temperature superpose accurately. This behavior can be seen in Fig. 1 for *atactic* polypropylene [16].

The proceeding statements concerning the effect of temperature on the behavior of polymers can be extended to pressure, although rheological data are extremely sparse. Dielectric spectroscopy is not a rheological probe *per se*; however, for polymers with a dipole moment parallel to the chain contour (“type-A” polymers), the dielectric normal mode is determined by the motion of the end-to-end chain vector [17,18]. This means that in the usual case where the dipole moment is weak so that dipole–dipole correlations are negligible, the dielectric response of a type-A polymer can yield the terminal relaxation time, the shape of the terminal relaxation function, and how these vary with thermodynamic variables such as temperature and pressure. Dielectric measurements are especially useful for the latter, since the absence of moving parts facilitates the experiment in comparison to mechanical

E-mail address: mike.roland@nrl.navy.mil

1359-0286/$ - see front matter Published by Elsevier Ltd.
doi:10.1016/j.cossms.2008.04.002

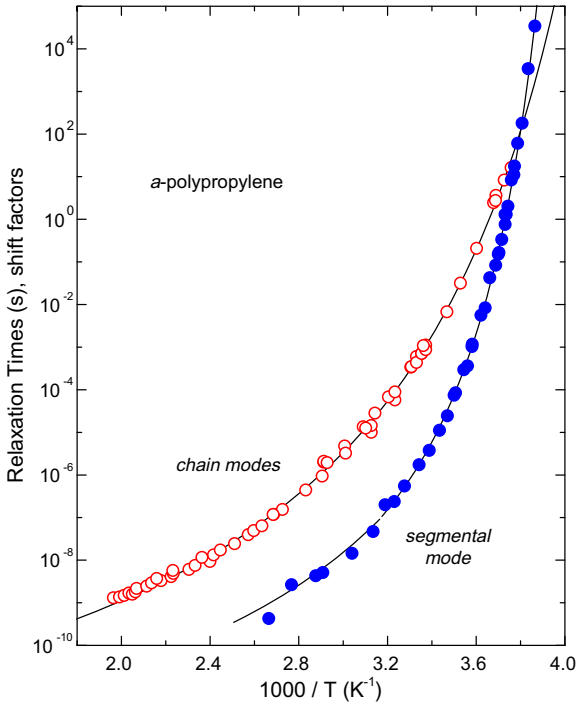

Fig. 1. Local segmental relaxation times (solid symbols) and time-temperature shift factors for the terminal relaxation (open symbols) for *atactic* polypropylene [16]. The data encompass measurements from dynamic mechanical spectroscopy, transient creep compliance, viscosity, dynamic light scattering, dielectric relaxation, and ^{13}C NMR. Vertical shifts were applied to the chain mode data to obtain superpositioning, so that the absolute position on the ordinate scale is arbitrary.

measurements [19]. In this review, we describe recent results addressing how temperature and pressure, and in turn volume, underlie the chain dynamics. Notwithstanding the breakdown of time-temperature (or time-pressure) superpositioning, general patterns emerge between the segmental and the chain dynamics, which can be connected to the forces between molecules. There is no universality of the chain dynamics, since these forces are governed by the intermolecular potential, which depends on the chemical structure. However, a simple scaling law, with predictive capability, is shown to be applicable to the dynamics of polymers over the very broad range of their viscoelastic response.

2. Scaling law and universality

The break down of time-temperature superpositioning precludes any correspondence between time-temperature shift factors for the segmental versus the global chain motion, even for a single material. The only exception is well above T_g, where Arrhenius curves of the relaxation times flatten and become parallel [16]. Comparing different materials, the chain dynamics exhibit similar features, such as molecular weight dependences and the shape of the relaxation function [2,6], since the coarse-graining appropriate to the large length scales diminishes the influence of the local chemical structure. However, the temperature dependence of the terminal relaxation time, τ_n, and viscosity, η, varies among different polymers, implying different local friction factors. Interestingly, Sokolov et al. [20–22] recently produced master curves of the shift factors for τ_n and η of various polymers plotted versus T_g/T, suggesting the existence of a universal T_g-normalized temperature dependence of the chain dynamics. This is an intriguing result, implying that a parameter, T_g, related to the local

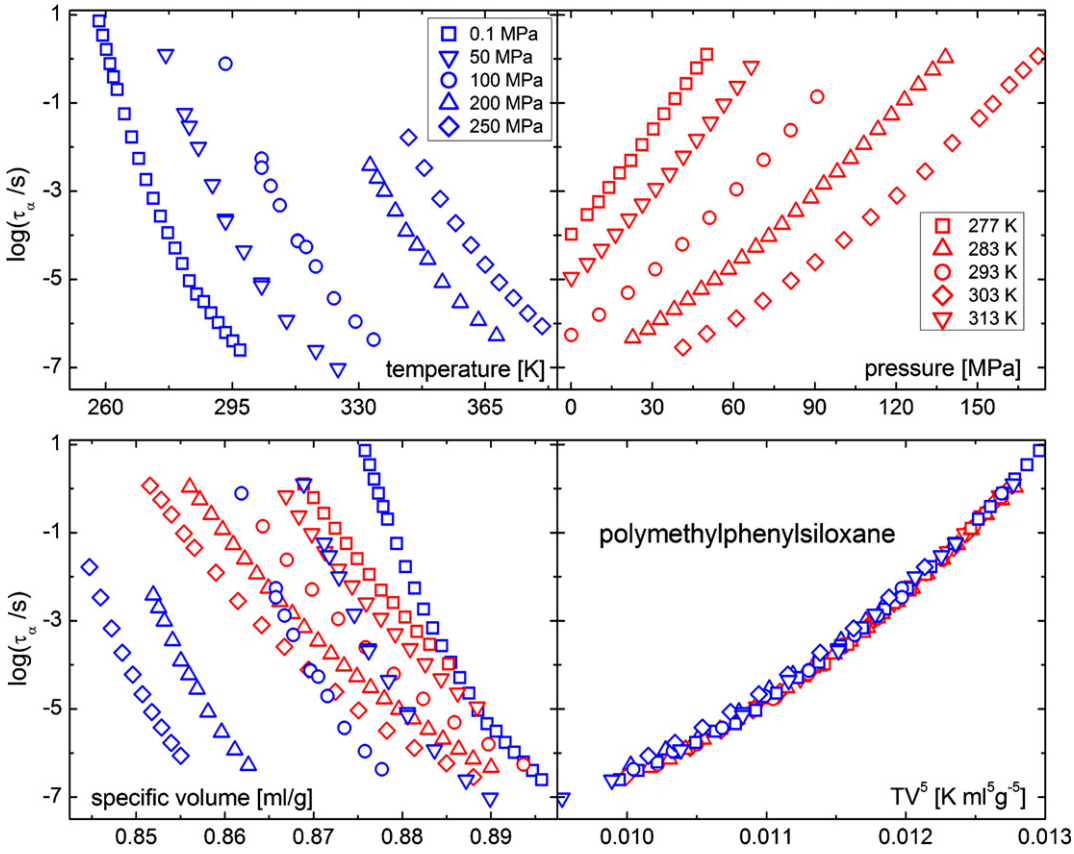

Fig. 2. Local segmental relaxation times of polymethyltolylsiloxane measured dielectrically: (upper left) as a function of temperature at the indicated pressures [29]; (upper right) as a function pressure at the indicated temperatures [29]; (lower left) data replotted as a function of specific volume; (lower right) superpositioning according to Eq. (2) with $\gamma = 5$ [30].

segmental dynamics can account for differences in the global dynamics. While many polymers conform at least approximately to this universal behavior, it turns out that variations in the T_g-scaled chain dynamics are evident for a number of materials [23].

The local segmental dynamics directly reflect the forces between segments, and since these forces are governed by the chemical structure, the segmental relaxation properties differ significantly among polymers. A common method of comparing the temperature behavior of the segmental relaxation time is the use of T_g-normalized Arrhenius curves. The slope at T_g

$$m = T_g^{-1}\left.\frac{d\log\tau_\alpha}{dT^{-1}}\right|_{T_g} \quad (1)$$

is called the "fragility" [24], which for polymers fall in the range from $46 \leqslant m \leqslant 191$ [25], corresponding to (very large) apparent activation energies, ~180–1200 kJ/mol. The fragility is known to correlate with other properties, such as the breadth of the relaxation dispersion [25] and the separation in time of the segmental and secondary relaxation processes [26].

The above consideration of T-dependences is restricted to constant (ambient) pressure; extension to the effect of pressure or volume on the dynamics complicates matters. The fragility, for example, decreases with pressure, in the absence of structural changes such as H-bond concentration [27], while the isochoric fragility is independent of temperature [27]. A means to classify the material response to changes in T and P is to express the segmental relaxation times as a function of the product variable TV^γ; that is [28]

$$\tau_\alpha = f(TV^\gamma) \quad (2)$$

in which V is specific volume and γ a material constant. This variable defines the relaxation time, so that a plot versus TV^γ of τ_α for a given polymer measured over a range of T and P will superpose to a single, material-specific master curve. This scaling, illustrated in Fig. 2 for a siloxane polymer [29,30], is quite general, having been demonstrated for more than 50 materials [19]. The exponent γ varies from 1.3 to 5.6 [19], reflecting the different influence of volume, relative to temperature, on the local dynamics of different polymers.

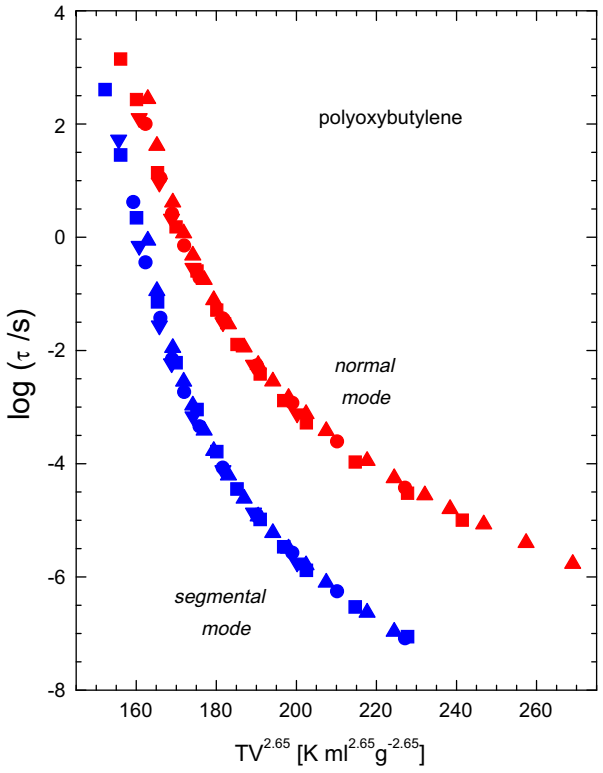

Fig. 3. Dielectric relaxation times for local segmental (lower) and normal mode (upper) for polyoxybutylene: isobars ($P \leqslant 628$ MPa) at 247 K (inverted triangles), 273 K (circles), and 297 K (triangles) and an isotherm (197–274 K) at 0.1 MPa (squares) [32].

Interestingly, when this scaling is extended to the chain dynamics of polymers, as measured by the dielectric normal mode in type-A polymers, the chain relaxation times for a given material also superpose to a single master curve versus TV^γ. Moreover, the scaling exponent γ has the identical value as for the segmental relaxation times, as shown for polypropylene glycol [31], 1,4-polyisoprene [31], and polyoxybutylene (POB) [32]. A similar result was found in molecular dynamic simulations of polybutadiene [33]. The equivalence of the scaling exponent for the segmental and global dynamics arises from the fact that both reflect the magnitude of the local friction coefficient. However, in the same manner that the T-dependence of the two modes differ, as discussed above, τ_α varies more strongly with TV^γ than does τ_n. Data for POB [32] showing this behavior are seen in Fig. 3. An explanation for the fact that the segmental and normal mode relaxation times are both functions of TV^γ with the same γ, yet have a difference dependence, is offered by the coupling model [34].

Eq. (2) has been derived from entropy considerations [35], leading to a connection between γ and the Grüneisen parameter [36]. Fundamentally the intermolecular potential governs the molecular motions, so that this exponent must be related to the steepness of the potential. For real materials the latter is difficult to quantify, but recent progress has been made by molecular dynamic simulations (mds).

3. Intermolecular potential

Molecular dynamic simulations of the motion of liquids near T_g commonly employ a Lennard–Jones (LJ) potential to describe the interactions between molecules [37]

$$U(r) = 4\varepsilon\left[\left(\frac{\sigma}{r}\right)^n - \left(\frac{\sigma}{r}\right)^6\right] \quad (3)$$

in which r is the intermolecular distance, ε and σ are material constants, and the repulsive exponent n is usually assumed to be 12. For polymers an additional harmonic potential is invoked to account for the intrachain forces [38,39]

$$U(r) = 4\varepsilon\left[\left(\frac{\sigma}{r}\right)^n - 2\left(\frac{\sigma}{r}\right)^6\right] + k(r-l)^2 \quad (4)$$

in which k is the backbone force constant and l the bond length. By applying the scaling relation to simulation data, the connection between the exponent γ and the intermolecular potential can be examined. In fact, by approximating the weak, long-range attractive forces as a spatially uniform background term, Eq. (3) simplifies to a repulsive inverse power law [37]

$$U(r) \sim r^{-n} + \text{const} \quad (5)$$

When Eq. (5) is applicable, all thermodynamic properties become a function of r^n or, equivalently $V^{n/3}$ [40]. This implies that $n/3$ can be identified with γ. This was borne out in early work that showed approximate collapse using $\gamma = 4$ of viscosity [41] and diffusion [42] data for LJ fluids with $n = 12$. This connection between the steepness of the repulsive potential and the scaling exponent was investigated further in mds of an LJ liquid in which the exponent of the repulsive term of the potential was varied between 8 and 36 [43]. The calculated diffusion constant conformed to the scaling law (Eq. (2)) with the exponent approximately equal to, but systematically larger than, one-third the value of n, the exponent in the repulsive potential. These results, shown in Fig. 4, confirm the connection of the dynamics and its scaling to the repulsive forces between molecules.

To understand why $\gamma > n/3$ requires consideration of the actual shape of the repulsive part of the potential, specifically the effect of the longer-range attractive term in Eq. (3). Shown in Fig. 5 is a representative plot of the intermolecular potential function for $n = 24$, along with the corresponding radial distribution function, $g(r)$ [43]. (The radial distribution function gives the probability of finding a particle at a distance r from another particle; thus, $g(r)$, describes the effect of intermolecular correlations on the distribution of molecules resulting from the forces between them.) It is seen in Fig. 5 that only at very small interparticle distances is the asymptotic region $U(r) \sim r^{-n}$ attained. At more accessible values of r, close to the minimum in the potential, the potential is steeper. In fact fitting the potential to a power law (Eq. (5)) in the range between $0.95r_{min}$ and $1.01r_{min}$, where r_{min} represents the interparticle separation at the minimum in $U(r)$, yields an n essentially equal to 3γ (see Table 1) [43]. This range of r corresponds to the distant of closest approach, as seen in the plot of the radial distribution function in Fig. 5. Budzien et al. [39] also found that inclusion of an attractive term in their simulations increases the value of γ that yields superposition of diffusion data.

These results underscore the idea that the scaling exponent provides direct information about the forces between molecules, in particular in the range of intermolecular separations important for the liquid (or melt) state. The steepness of the repulsive poten-

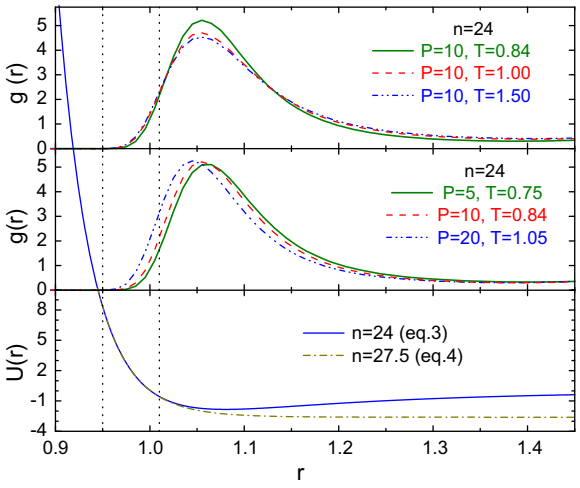

Fig. 5. (top) Radial distribution functions for $P = 10$ at the three indicated temperatures of an LJ fluid (Eq. (3)) with a repulsive exponent = 24; (middle) radial distribution function for the three indicated pressures at the lowest equilibrated temperatures; (bottom) pair potential (solid line) and best-fit IPL (Eq. (5), dash-dotted line) in the range $0.95 \leqslant r \leqslant 1.01$ (indicated by the vertical lines in all panels) from Ref. [43].

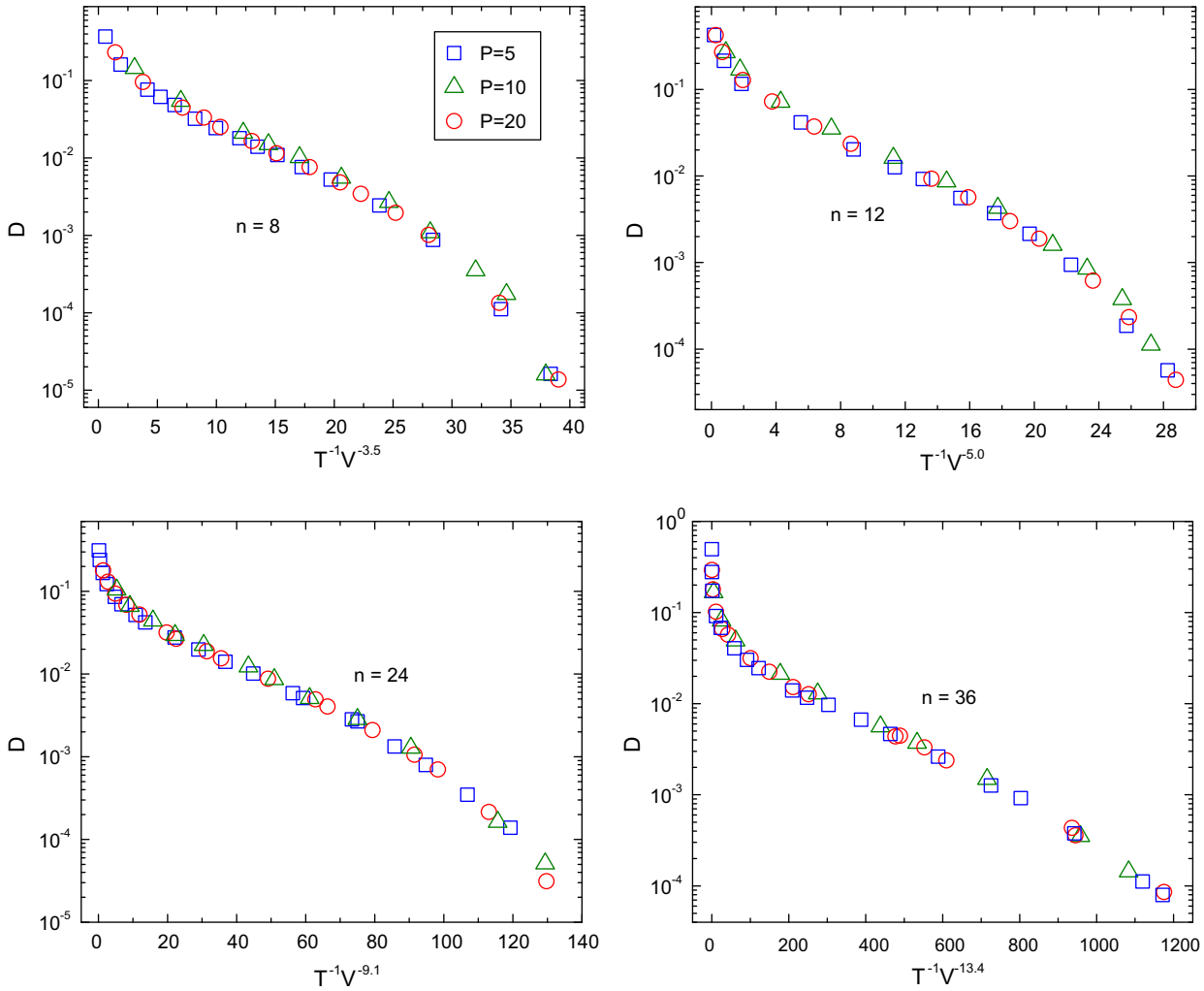

Fig. 4. Diffusion coefficients for three pressures and a range of temperatures from simulations using the indicated values of the repulsive exponent (Eq. (3)) [43]. Note that the ordinate is the diffusion constant normalized by $V^{1/3}T^{1/2}$, but the superpositioning is very similar without the normalization.

Table 1
Exponents from mds of LJ fluid [43]

n	$n(0.95 < r/r_{min} < 1.01)$	3γ
8	10.9	10.5
12	14.9	15
24	27.2	27.3
36	39.9	40.2

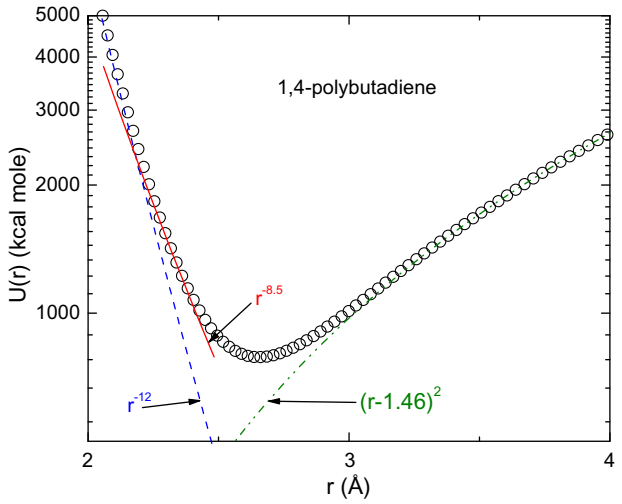

Fig. 6. Intermolecular potential (circles) calculated using Eq. (4) with $n = 12$ and average values as indicated for the other parameters of 1,4-polybutadiene [46]. The LJ intermolecular (dashed line) and harmonic intramolecular (dashed-dotted line) components are shown, along with the power law (solid line) having a slope equal to the three times the value of the γ that superposed the segmental and chain relaxation times [33].

tial exerts a dominant role in governing the dynamic behavior. However, as stated above, the high concentration of intramolecular bonds in chain molecules means that the intramolecular forces make a substantial contribution. Since intramolecular interactions do not change much with pressure (chains simply move closer together rather than change their radius of gyration) [32], volume effects *per se* tend to be weaker in polymers than molecular liquids [44,45]. This effect of the intramolecular bonds was evident in mds of Tsolou et al. [33] on 1,4-polybutadiene. Using Eq. (4) to describe the potential with $n = 12$, relaxation times, for both the segmental and terminal chain dynamics, superposed when plotted according to Eq. (2). The scaling exponent collapsing the various $\tau(T,V)$ data, $\gamma = 2.8$, is *less* than one-third the value of the repulsive exponent. This is opposite to the results for simple LJ particles (Fig. 5) [43], for which the scaling exponent is *larger* than $n/3$.

To understand this in Fig. 6 we plot $U(r)$ calculated using representative values for polybutadiene: $\varepsilon = 4.12$ kJ/mol, $\sigma = 4.19$ Å, $k = 3.4$ MJ/(molÅ^2), and $l = 1.46$ Å [46]. Similar to the data in Fig. 5, in the limit of small r, $U(r)$ has a power law form with a slope equal to 12. However, nearer the minimum the potential is flatter. The line in the figure is for $U(r) \sim r^{-8.5}$, which corresponds to one-third the γ yielding superposition of the diffusion data. Thus, the presence of the harmonic term, due to chain stretching and bending motions, softens the effective potential. This result is in keeping with the general observation that volume changes exert a weaker effect on the dynamics of polymers than on the motion of small molecules [19,44,45].

4. Summary

The defining aspect of polymers – the giant size of their constituent molecules – gives rise to relaxation properties not seen in simple molecules. Polymer dynamics encompass a range of length scales, with motions at the various length scales responding differently to changes in thermodynamic variables (T, P, and V). This causes the well-known breakdown of time-temperature superpositioning in the glass transition zone, where both the chain and segmental modes contribute. Nevertheless, relaxation times for both the global chain and local segmental modes collapse onto (different) respective master curves as a function of the scaling variable TV^γ, for the same value of the exponent γ. Similar to the greater sensitivity of the segmental modes to changes in T, P, and V, τ_α vary more strongly with TV^γ than do τ_n, notwithstanding the equivalent values of γ for the two modes. Molecular dynamics simulations bring out the fact that the magnitude of this scaling exponent reflects the steepness of the intermolecular repulsive potential in the vicinity of the minimum, where the fluctuating segments spend most of their time. The contribution of intramolecular bonds softens the effective potential, leading to smaller values of γ. This weaker influence of volume in polymers compared to molecular liquids is ironic, given the long-standing reliance on free volume concepts in the interpretation of the physical properties of polymers.

Aside from insights into the intermolecular potential, the scaling relation has practical utility. If the temperature dependence of the relaxation times is known for ambient pressure (the usual case), any arbitrary combination of T and P can be calculated from the equation of state that will correspond to the ambient pressure T and V. The two thermodynamic conditions (ambient and elevated P) will have the same relaxation time, since they have the same product variable TV (*viz.* Eq. (2)). Thus, for any measured τ_α or τ_α, all thermodynamic conditions associated with the same value of relaxation time can be calculated by using the scaling relationship. The only requirement is knowledge of the equation of state. The approach has been verified and used to explore the dynamics of various glass-forming liquids over a range of conditions [27].

Acknowledgement

Stimulating discussions with R. Casalini, K.L. Ngai, and D. Coslovich are gratefully acknowledged. This work was supported by the Office of Naval Research.

References

[1] de Gennes PG. J Chem Phys 1971;55:572.
[2] Doi M, Edwards SF. The theory of polymer dynamics. Oxford University Press; 1986.
[3] Lodge TP, Rotstein NA, Prager S. In: Prigogine I, Rice SA, editors. Adv Chem Phys. John Wiley and Sons; 1990.
[4] Adachi K, Kotaka T. Polym Yearbook 1990;6:43.
[5] Watanabe H. Prog Polym Sci 1999;24:1253.
[6] Ferry JD. Viscoelastic properties of polymers. Wiley; 1980 [chapter 10].
[7] Plazek DJ. J Phys Chem 1965;6:612.
[8] Plazek DJ. Polym J 1980;12:43.
[9] Ngai KL, Schonhals A, Schlosser E. Macromolecules 1992;25:4915.
[10] Plazek DJ, Bero C, Neumeister S, Floudas G, Fytas G, Ngai KL. Coll Polym Sci 1994;272:1430.
[11] Santangelo PG, Roland CM. Macromolecules 1998;31:3715.
[12] Robertson CG, Rademacher CM. Macromolecules 2004;37:10009.
[13] Plazek DJ, Chay I-C, Ngai KL, Roland CM. Macromolecules 1995;28:6432.
[14] Santangelo PG, Ngai KL, Roland CM. Macromolecules 1996;29:3651.
[15] Yamane M, Hirose Y, Adachi K. Macromolecules 2005;38:10686.
[16] Roland CM, Ngai KL, Santangelo PG, Qiu XH, Ediger MD, Plazek DJ. Macromolecules 2001;34:6159.
[17] McCrum NG, Read BE, Williams G. Anelastic and dielectric effects in polymeric solids. Dover Publications; 1967.
[18] Kremer F, Schohals A, editors. Broadband dielectric spectroscopy. Springer-Verlag; 2003.
[19] Roland CM, Hensel-Bielowka S, Paluch M, Casalini R. Rep Prog Phys 2005;68:1405.
[20] Ding Y, Sokolov AP. Macromolecules 2006;39:3322.
[21] Sokolov AP, Hayashi Y. J Non-Cryst Solids 2007;353:3838.
[22] Liu CY, He JS, Keunings R, Bailly C. Macromolecules 2006;39:8867.
[23] Ngai KL, Plazek DJ, Roland CM. Macromolecules 2008;41.
[24] Angell CA. J Non-Cryst Sol 1991;131–133:13.

[25] Böhmer R, Ngai KL, Angell CA, Plazek DJ. J Chem Phys 1993;99:4201.
[26] Ngai KL. J Chem Phys 1998;109:6982.
[27] Casalini R, Roland CM. Phys Rev B 2005;71:014210.
[28] Casalini R, Roland CM. Phys Rev E 2004;69:062501.
[29] Paluch M, Pawlus S, Roland CM. Macromolecules 2002;35:7338.
[30] Casalini R, Roland CM. Coll Polym Sci 2004;283:107.
[31] Roland CM, Casalini R, Paluch M. J Polym Sci Polym Phys Ed 2004;42:4313.
[32] Casalini R, Roland CM. Macromolecules 2005;38:1779.
[33] Tsolou G, Harmandaris VA, Mavrantzas VG. J Chem Phys 2006;124:1084906.
[34] Ngai KL, Casalini R, Roland CM. Macromolecules 2005;38:4363.
[35] Casalini R, Mohanty U, Roland CM. J Chem Phys 2006;125:014505.
[36] Roland CM, Feldman JL, Casalini R. J Non-Cryst Solids 2006;352:4895.
[37] March NH, Tosi MP. Introduction to liquid state physics. World Scientific; 2002.
[38] Tsolou G, Mavrantzas VG, Theodorou DN. Macromolecules 2005;38:1478.
[39] Budzien J, McCoy JD, Adolf DB. J Chem Phys 2004;121:10291.
[40] Hoover WH, Ross M. Contemp Phys 1971;12:339.
[41] Ashurst WT, Hoover WG. Phys Rev A 1975;11:658.
[42] Bernu B, Hansen JP, Hiwatari Y, Pastore G. Phys Rev A 1987;36:4891.
[43] Coslovich D, Roland CM. J Phys Chem B 2008;112:1329.
[44] Paluch M, Casalini R, Roland CM. Phys Rev B 2002;66:092202.
[45] Roland CM, Paluch M, Pakula T, Casalini R. Philos Mag 2004;84:1573.
[46] Roland CM, Bair S, Casalini R. J Chem Phys 2006;125:124508.